JOURNAL OF APPLIED ELECTROCHEMISTRY 17 (1987) 1021–1036

Influence of methylcellulose-coated paper separators on the corrosion, polarization and impedance characteristics of zinc in concentrated ammonium chloride solution. I. Behaviour in flooded electrolyte

L. M. BAUGH*, N. C. WHITE

Ever Ready Ltd, Technical Division, Tanfield Lea, Stanley, Co. Durham, UK

Received 6 March 1986; revised 16 January 1987

The corrosion characteristics of both pure and amalgamated zinc have been studied in 6.0 M NH_4Cl using steady-state polarization and a.c. impedance methods, and the influence of methylcellulose-coated and uncoated paper separators have been determined. Irrespective of the type of separator present, the results can be interpreted almost exclusively in terms of charge-transfer effects. In the presence of the base paper the anodic zinc dissolution process is inhibited by 79% whilst the rate of cathodic hydrogen evolution is inhibited by only 43%. Similarly, in the presence of the complete methylcellulose-coated separator formulation the anodic reaction is inhibited by 98–99% whilst the cathodic reaction is inhibited by only 60–74%. In either case it is shown that the anodic inhibition is considerably greater than that expected on the basis of a simple blocking type model, whereas the cathodic inhibition is considerably less. Evidence is presented which suggests that the excessive inhibition of the anodic current is a consequence of the specific influence of the separator on the stability and adsorption behaviour of Zn(I) intermediates in the zinc dissolution reaction. It is also postulated that the deficient inhibition of the cathodic current may result from the small size and high mobility of the proton which allows it to penetrate those regions of the metal–separator interface normally inaccessible to bulkier ions.

Overall, the corrosion-inhibiting efficiency of the base paper is 41% whilst that of the complete methylcellulose-coated paper separator formulation is 70–75%. These results reflect a substantial influence of the separator material on the corrosion behaviour of zinc.

Nomenclature

General

m measured (superscript or subscript)
c calculated (superscript or subscript)

Ohmic impedance terms and derived parameters

A_e^m measured area fraction of electrolyte assuming $A_e^m = V_e^m/\theta_m$
A_e^c calculated area fraction of electrolyte assuming $A_e^c = V_e^c/\theta_c$
l average length of pores in separator
r_c resistance of electrolyte within the coating layer
r_e resistance of 'free' electrolyte having an equivalent thickness and geometry of that of the free base paper or coating layer

* *Present address*: BNF Metals Technology Centre, Grove Laboratories, Denchworth Road, Wantage, Oxon, UK.

0021–891X/87 $03.00 + .12 © 1987 Chapman and Hall Ltd.

r_p resistance of electrolyte within the base paper
r_s resistance of electrolyte within the base paper *or* coating layer
R_Ω total resistance of electrolyte between Luggin probe and zinc surface in the absence of a separator
R_Ω^p total resistance of electrolyte between Luggin probe and zinc surface in the presence of the base paper only
R_Ω^s total resistance of electrolyte between Luggin probe and zinc surface in the presence of the coated paper separator
t_c thickness of coating layer ($t_c = 30\,\mu m$)
t_p thickness of base paper ($t_p = 185\,\mu m$)
V_e^m measured volume fraction of electrolyte in the separator
V_e^c calculated volume fraction of electrolyte in the separator assuming $r_s/r_e = 1/V_e^3$
x constant distance between zinc surface and Luggin probe (absence of separator) or between Luggin probe and free electrolyte exposed (outer) separator surface (presence of separator) ($x = 0.10\,cm$)
θ_m measured (experimentally derived) tortuosity factor assuming measured volume fraction V_e^m and relation $r_s/r_e = \theta^2/V_e^m$
θ_c calculated tortuosity factor assuming $\theta = 1/V_e^c$
ϱ resistivity of free electrolyte
$\bar{\varrho}$ resistivity of the separator

Polarization terms and parameters derived from high-current data

b_a anodic Tafel slope (mV per decade)
b_c cathodic Tafel slope
i_a anodic current in the Tafel region
i_c cathodic current in the Tafel region
i_a^s anodic current in the Tafel region in the presence of the separator
i_c^s cathodic current in the Tafel region in the presence of the separator
i_{cor}^{ext} corrosion current derived by extrapolation of anodic and cathodic current–potential data
I_s current inhibition (%) due to the separator
$\Delta\eta$ shift in overpotential produced by the separator
ϕ_e area fraction of electrolyte adjacent to the zinc surface calculated assuming a 1 : 1 correlation between separator coverage and current inhibition
ϕ_p area fraction of solid (polymer) adjacent to the zinc surface assuming a 1 : 1 correlation between separator coverage and current inhibition

Polarization and impedance terms and parameters derived from low-current data

C_{dl} double-layer capacity
E_{cor} corrosion potential
$i_{cor}^{R_{dc}}$ corrosion current derived from R_{dc} value
$i_{cor}^{R_p}$ corrosion current derived from R_p value
i_{cor}^{bat} battery corrosion current derived by extrapolation of cathodic Tafel line back to zinc potential in complete Leclanché electrolyte
I_{cor} corrosion current inhibition
I_{cor}^{bat} battery corrosion current inhibition
R_{ct} charge-transfer resistance
R_{dc} direct current resistance extrapolated from impedance data $(Z)_{\omega=0}$
R_p polarization resistance $(dE/di)_{i\to 0}$

1. Introduction

During the long-term storage of Leclanché cells, corrosion of the zinc anode may be appreciable leading to poor capacity retention. This has prompted several fundamental studies designed to elucidate more clearly the factors responsible in order that remedial action can be taken. Previous investigations into zinc corrosion mechanisms conducted by Ever Ready Ltd have included a study of the effects of ionic composition [1, 2], the cause of pitting during discharge [3, 4], the role of amalgamation [5, 6], and the influence of alloying constituents [7]. An important factor neglected in these earlier studies, however, was the effect of the separator present in complete Leclanché cells adjacent to and in contact with the zinc anode. This would also be expected to participate in determining the overall corrosion characteristics of zinc. Whilst the influence of the methylcellulose-coated separator on the *zinc exchange* reaction in Leclanché electrolyte has already been studied [8], little information is available concerning its effect on *corrosion* behaviour. The present communication therefore focuses attention upon the latter. Potentiostatic polarization and a.c. impedance techniques have been applied to the study of both pure zinc and amalgamated zinc electrodes corroding in Leclanché related (6.0 M NH_4Cl) electrolyte in the presence and absence of the separator. A comparison of the present results with those obtained in the complete battery environment will be published in Part II [9].

2. Experimental details

2.1. *Materials and electrode preparation*

Pure zinc rods of diameter 6 mm (Koch-Light, purity 99.9999%) were sheathed in tightly fitting Teflon and prepared as discussed previously [1] except that they were not chemically etched. The standard separator material consisted of a base paper (α-cellulose) of $100\,g\,m^{-2}$ and thickness $185\,\mu m$ having a methylcellulose coating on one side of $30\,g\,m^{-2}$ and thickness $30\,\mu m$. The structural formula of methylcellulose is shown below

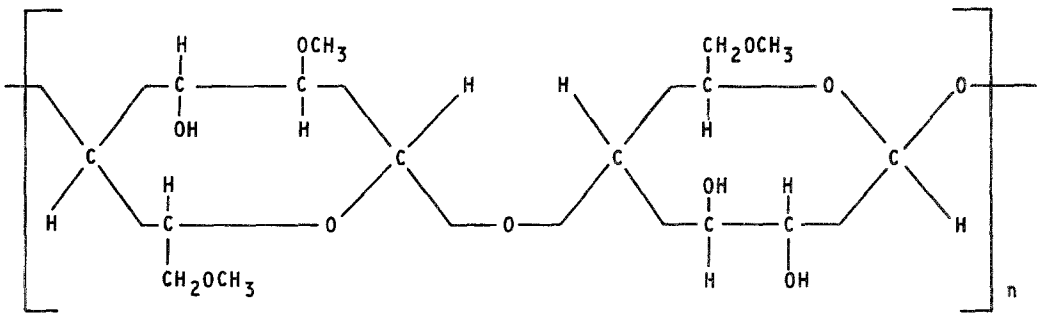

Separator papers were held in contact with the working electrode surfaces using a Teflon holder which fitted around the rim of the working electrode sheath only, thus permitting direct access of electrolyte to the metal–separator interface.

Amalgamation was achieved by holding a disc of the calomel impregnated methylcellulose-coated separator ($157\,\mu g\,Hg\,cm^{-2}$) in contact with the electrode using the special Teflon holder. The electrode–separator–holder system was orientated to form a cup facing upwards into which electrolyte could be placed. The separator was wetted with working electrolyte. A disc of plain base paper was then placed in contact with the methylcellulose-impregnated paper and the Teflon holder recess was filled with working electrolyte gelled with methylcellulose. Such an arrangement was devised to prevent the separator crinkling and lifting off the zinc surface due to over-wetting. Gelling the electrolyte also served to establish conditions similar to those encountered in the complete cell

during amalgamation, i.e. limited electrolyte volume in contact with the separator. Electrodes were left to equilibrate for 20 h after which the gelled electrolyte layer and base paper disc were removed. This method of amalgamation produced electrodes which showed no signs of ageing [5, 6] over the following 24 h period.

2.2. *Cell, electrode assemblies and solutions*

The electrochemical cell, electrode assemblies and instrumentation have been described previously [1]. The reference electrode was $Hg/Hg_2Cl_2/KCl(sat)$. Determination of separator resistances from high-frequency ohmic impedance measurements was facilitated by maintaining the distance of the Luggin capillary probe at a *constant* distance of 0.10 cm from either the zinc surface (experiments without separators) or the free electrolyte exposed (outer) separator surface (experiments with separators).

The 6 M NH_4Cl solutions were prepared from recrystallized AnalaR grade NH_4Cl using thrice-distilled water.

2.3. *Procedure*

Current–potential data were recorded by monitoring the current at fixed potential increments during slow potential sweeps (5 mV min^{-1}). The general procedure and impedance measuring technique have been described previously [1]. The method of determining volume fractions and tortuosity factors for the separators from ohmic impedance data is described in the Appendix. An experimental value for the mean volume fraction of the base paper was determined using a density of 1.66 g cm^{-3} [10].

3. Results and discussion

3.1. *General*

In NH_4Cl solutions polarization and impedance characteristics for zinc reflect corrosion processes [2]. The polarization curves consist of an anodic branch due to zinc dissolution, a cathodic branch resulting from hydrogen evolution and impedance characteristics at the open circuit (corrosion) potential which are directly quantifiable in terms of the net corrosion rate of the metal. The overall component reactions which contribute towards the net corrosion process can be represented by

$$Zn + nCl^- \rightleftharpoons ZnCl_n^{2-n} + 2e \qquad \text{anodic} \qquad (1)$$

$$2NH_4^+ + 2e \longrightarrow 2NH_3 + H_2 \qquad \text{cathodic} \qquad (2)$$

$$Zn + 2NH_4^+ + nCl^- \longrightarrow ZnCl_n^{2-n} + 2NH_3 + H_2 \qquad \text{net} \qquad (3)$$

Here, the cathodic reactants are NH_4^+ ions, but this does not preclude the possibility that prior dissociation occurs to form protons which may well be the directly electroactive species [2].

It is clear that any change in the rate of the corrosion reaction 3 resulting from the presence of a separator adjacent to the zinc will depend upon the extent to which the separator material induces changes in the individual reactions 1 and 2. This in turn will depend upon the exact mechanisms of these reactions and the nature of the chemical species involved. A knowledge of these mechanisms in the *absence* of the separator is therefore important. Furthermore, the surface condition of the metal and in particular the state of surface amalgamation will also play a role.

3.2. *Electrochemical Data*

Fig. 1 illustrates the electrochemical data for pure zinc in the absence and presence of either the base

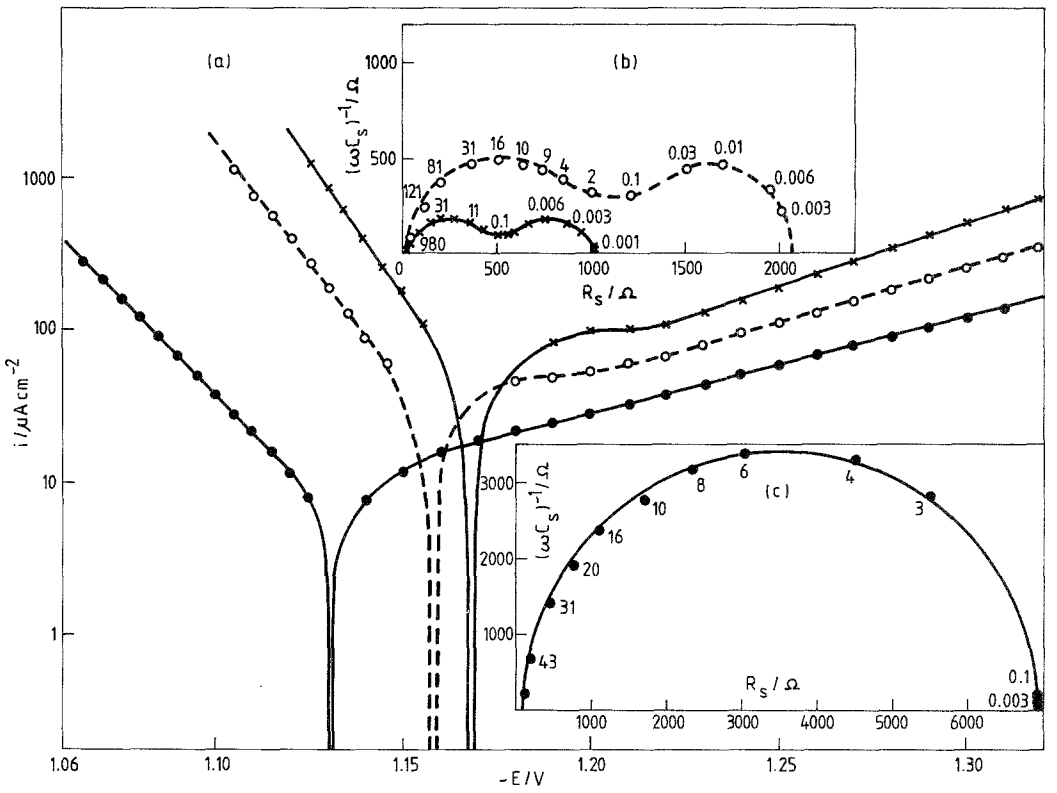

Fig. 1. Effect of the separator on the polarization and equilibrium impedance characteristics (50 kHz–3 mHz) of pure zinc in 6 M NH_4Cl. (a) Polarization characteristics, (×) in the absence of a separator, (O———O) in the presence of the base paper only, (●) in the presence of the complete separator (methylcellulose–paper) formulation. (b) Impedance spectra, (×) in the absence of a separator, (O———O) in the presence of the base paper only. (c) Impedance spectrum in the presence of the complete separator formulation.

paper or the complete separator formulation, i.e. base paper + methylcellulose coating. Fig. 1a shows polarization curves over a range of potentials and Fig. 1b and 1c complex impedance diagrams (inset) determined at the open-circuit potential in respect of the systems zinc–paper and zinc–methylcellulose–paper, respectively. In agreement with earlier work [2, 5] the slope of the anodic polarization line in the absence of any separator is close (within 2 mV) to 30 mV per decade ($2.3RT/2F$), indicative of a reversible (Nernstian) two-electron dissolution–deposition process which is jointly controlled by charge transfer and mass transfer. Proof of participation by the latter was obtained by observing a rotation speed dependence of the anodic current [5]. The same result was observed in the case of zinc dissolution in concentrated alkaline solution where the 30 mV slope* was also derived theoretically [11]. The influence of the base paper is to produce an almost parallel shift in the polarization line to lower current values. In fact, the resulting slope is exactly 30 mV per decade. Similarly, the slope of the cathodic polarization line in the absence of any separator is 120 mV per decade ($2.3RT/\alpha nF$, $\alpha = 0.5$) indicative of a charge transfer-controlled hydrogen evolution process. The influence of the base paper is again to shift the polarization line to lower current values but at the same time increasing the Tafel slope slightly to 140 mV per decade. Such increases in cathodic slope can also be induced by amalgamation and may possibly be interpreted either in terms of increasing heterogeneity, as in the case of the Zn–KOH system [5], or the

* It is important to recognize that these slopes are not 'Tafel' slopes but 'Nernst' slopes, since the former cannot have any dependence on rotation speed.

increasing presence of a semi-conducting oxide film [6]. The impedance diagrams of Fig. 1b are qualitatively and quantitatively in agreement with this interpretation. In the absence of any separator the impedance consists of a high-frequency semicircle indicative of a charge-transfer process followed at low frequencies by a shape which is consistent essentially with a rapidly relaxing Warburg impedance. This reflects some diffusion control in the net corrosion process and can be attributed to the anodic reaction. The influence of the base paper is to simply increase the size of the diagram by a factor of about two, which is consistent with an inhibiting effect on the zinc corrosion rate of 50%. Corrosion-inhibiting efficiencies will be discussed more quantitatively later in the paper.

Although the above changes induced by the presence of the base paper might be regarded as relatively minor, much more significant changes occur when the *complete* separator formulation is adjacent to the zinc. Fig. 1a shows that this comment applies particularly in the case of the anodic dissolution process where the current is reduced by over two orders of magnitude. Furthermore, the slope of the anodic polarization line changes from 30 to 40 mV per decade. The latter is consistent with a charge transfer-controlled dissolution mechanism consisting of two consecutive, one-electron transfers of the form

$$\text{step 1} \qquad \text{Zn} \rightleftharpoons \text{Zn(I)} + e \tag{4}$$

$$\text{step 2} \qquad \text{Zn(I)} \longrightarrow \text{Zn(II)} + e \quad \text{r.d.s.} \tag{5}$$

$$\text{overall} \qquad \text{Zn} \longrightarrow \text{Zn(II)} + 2e \tag{6}$$

where Zn(I) is an intermediate species and the second step (Equation 5) is rate-determining [12]. It should be emphasized that in this sequence, additional steps resulting from chemical equilibria between surface zinc species and Cl^- ions have been neglected, since the exact mechanism has not been resolved. However, by analogy with the situation in concentrated alkaline solution [13] at least two additional steps will probably occur. Thus it can be concluded from the anodic data in Fig. 1a that in the presence of the methylcellulose layer the rate of charge transfer is reduced to such an extent that the reaction ceases to be influenced in any way by mass transfer limitations. On the cathodic side of the polarization curves the methylcellulose layer again produces a shift, but much less significant than that on the anodic side. The slope of the Tafel line for hydrogen evolution is also increased to 160 mV per decade. These are important results because they demonstrate a considerable measure of specificity in the manner in which methylcellulose inhibits electrode processes. This is reflected in another way in Fig. 1a where it can be seen that the open-circuit potential is shifted by 39 mV in the anodic direction ($\Delta E_{cor} = +38$ mV), showing a clear preference for inhibition of the anodic zinc dissolution reaction 1 rather than the cathodic hydrogen evolution reaction 2. That mass transfer effects are not involved in determining either the anodic or the cathodic polarization characteristics in the presence of the complete separator formulation is confirmed by the impedance diagram shown in Fig. 1c determined at the corrosion potential. Here, in contrast with the zinc and zinc–paper cases of Fig. 1b, a *single* charge transfer semicircle is the only feature even at the lowest frequency studied (1 mHz).

Fig. 2 illustrates the electrochemical data for amalgamated zinc in the presence and absence of the complete separator formulation. In this case a simplification is evident. The anodic current potential plot consists of a Tafel line of slope 40 mV per decade even in the *absence* of the separator. The same slope has been observed on zinc amalgamated by an electrodeposition method [5]. A careful comparison of Figs 2a and 1a reveals that the polarization line for zinc (Hg) is considerably lower than that for pure zinc and this effect has also been noted and discussed in terms of a non-passivating layer on the amalgamated parts of the zinc surface [6]. Interestingly, the effect is not restricted to pure NH_4Cl solutions and has been observed in complete Leclanché electrolyte ($NH_4Cl + ZnCl_2$) [8]. The effect of the separator is to produce a parallel shift in the anodic Tafel

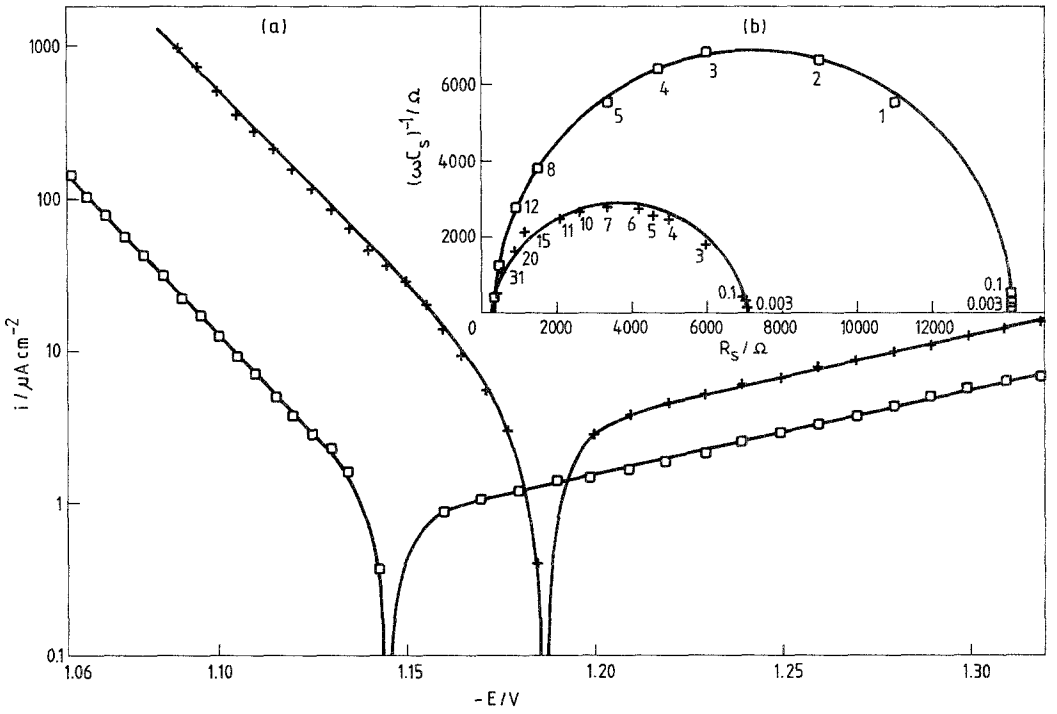

Fig. 2. Effect of the separator on the polarization and equilibrium impedance characteristics (50 kHz–3 mHz) of amalgamated zinc in 6 M NH_4Cl. (a) Polarization characteristics, (+) in the absence of a separator, (□) in the presence of the complete separator (methylcellulose–paper) formulation. (b) Impedance spectra, (+) in the absence of a separator, (□) in the presence of the complete separator formulation.

line to much lower current values. A similar parallel shift is observed in the cathodic line but to a lesser extent. Thus, again, only charge-transfer processes are important with a clear preference for the methylcellulose to inhibit the zinc dissolution reaction 1 rather than the hydrogen evolution process ($\Delta E_{cor} = +40$ mV). That mass transfer effects are not involved in determining the rates of these reactions, either in the presence or the absence of methylcellulose, is confirmed from the impedance diagrams shown in Fig. 2b where it is clear that charge transfer semicircles are the only feature even at the lowest frequencies studied (3 mHz).

The above conclusions point to quite specific effects of the separator on the rates of the charge-transfer reactions. However, the mechanism by which the separator can cause these changes has not been considered. Clearly, to a first approximation the primary mechanism will be through some kind of *blocking action*. In order to make further progress it is first necessary to estimate the likely blocking effect. This will be considered below.

3.3. *Separator parameters and correlation with polarization data*

As far as charge-transfer processes are concerned the pertinent parameter which must be established is the area fraction of the separator in contact with the zinc surface, A_p, or the directly related area fraction of electrolyte, A_e, where

$$A_p = 1 - A_e \tag{7}$$

The latter parameter can be deduced from the expression

$$A_e = V_e/\theta \tag{8}$$

where V_e is the volume fraction of the electrolyte in the separator and θ its tortuosity value. This expression is deduced from a simple pore model ('hose-pipe' model) in which the current flow at the electrode surface is perpendicular to the plane of the electrode itself. However, both V_e and θ must be known. These parameters are related to experimentally determinable resistance values via the equation [14]

$$r_s/r_e = \theta^2/V_e \tag{9}$$

where r_s is the resistance of the electrolyte within the separator and r_e is the resistance of free electrolyte having an equivalent volume and geometry to that of the separator. Simplification of Equation 9 follows if a particular model relating θ to V_e is assumed. Thus, using a gel-probability model [15] found to be applicable in the case of a Whatman's No 41 filter paper [16],

$$\theta = 1/V_e \tag{10}$$

and Equation 9 reduces to

$$r_s/r_e = 1/V_e^3 \tag{11}$$

Equations 7 to 11 can be used to estimate A_p in the case of a *gel layer* where V_e cannot easily be determined due to swelling etc. In the case of a paper separator in the absence of a gel layer, however, V_e is measureable. Thus, *two* values of V_e are determinable in the case of the paper separator: a measured value and a calculated value assuming Equation 11. This in turn leads to two different values of θ, A_e and A_p designated 'measured' and 'calculated'. The Appendix describes more fully the procedure adopted and in particular the method used to determine the relevant r_s and r_e values from the ohmic impedance data.

Table 1 summarizes the volume fraction, tortuosity and area fraction data. It can be seen that in the case of the zinc–paper system, measured and calculated volume fractions agree fairly well and hence the agreement between the tortuosity values is very good. These results prove that the gel-probability model represents a good description of the system in agreement with the earlier work of Agopsowicz *et al.* [16]. The absolute values of the volume fractions and tortuosity factors are also in reasonable agreement with the earlier work (0.56 and 1.9, respectively) despite the use of a different paper. The calculations lead to an area fraction for the solid, A_p, of 0.65–0.67. Thus, a blocking-type model for inhibition would predict that the electrode process should be inhibited by 66%. In order to compare this prediction with experiment, estimates of the degree of inhibition were obtained from expressions of the form

$$\phi_e = i^s/i \tag{12}$$

and

$$\phi_p = 1 - \phi_e = 1 - (i^s/i) \tag{13}$$

where ϕ_e is an inhibition factor which, in the simplest analysis, will be approximately equal to the

Table 1. Parameters derived from ohmic impedance data

Electrode–separator system	R_Ω ($\Omega\,cm^2$)	R_Ω^s ($\Omega\,cm^2$)	r_e ($\Omega\,cm^2$)	r_s ($\Omega\,cm^2$)	r_s/r_e	V_e^c	θ_c	A_e^c	A_p^c
Zn–paper	0.23	0.45	0.042	0.22	5.2	0.58	1.7	0.33	0.67
Zn–methylcellulose–paper	0.23	0.65	0.0069	0.20	29.0	0.33	3.1	0.11	0.89
Zn(Hg)–methylcellulose–paper	0.28	0.65	0.0084	0.20	23.8	0.35	2.9	0.12	0.88

Additional parameters used in calculations: $x = 0.10\,cm$; $t_p = 185\,\mu m$; $t_c = 30\,\mu m$.
Parameters derived for Zn–paper system assuming the directly *measured* value of V_e to pertain: $V_e^m = 0.65$; $\theta_m = 1.8$; $A_e^m = 0.35$; $A_p^m = 0.67$.

area fraction of the electrolyte adjacent to the metal; ϕ_p is an inhibition factor approximately equal to the area fraction of the solid (polymer) adjacent to the metal; i^s is the current flow in the Tafel region in the presence of the separator and i is the current at the same potential in the absence of the separator. The inhibition can be further represented as

$$I_s = 100\phi_p \tag{14}$$

Table 2 summarizes the data. The potentials at which the inhibition factors have been determined are indicated below the table. Also shown are values for the increase in polarization, $\Delta\eta$, produced by the separator at constant current density in the Tafel region. In the case of the zinc–paper system the measured inhibition efficiency is 79% for zinc dissolution and 43% for hydrogen evolution. Thus the anodic current inhibition is 13% *greater* than that predicted on the basis of a purely blocking-type mechanism (namely 66%) whilst the cathodic current inhibition is 23% *less*.

Table 1 shows that in the case of the zinc–methylcellulose–paper and Zn(Hg)–methylcellulose–paper systems there is very close agreement between the measured parameters as would be expected. The volume fractions and tortuosities refer to the methylcellulose layer only, as described in the Appendix. It can be seen that the volume fractions are approximately 50% less than those determined in the case of the paper, whilst the tortuosities are approximately twice as great. It must be re-emphasized, however, that the deductions in respect of the methylcellulose layer depend upon the applicability of the gel-probability model which has not been proved experimentally in the present study. Nevertheless, if this is accepted as a working hypothesis, then a meaningful comparison of the derived A_e and A_p values with the respective ϕ values of Table 2 can be made in the case of the methylcellulose layer. Indeed, if this is carried out, then a similar pattern emerges to that deduced for the paper separator alone. Thus, the inhibition is 98–99% for zinc dissolution compared with a predicted value of 88–89% deduced from the A_p values (Table 1), whereas the cathodic inhibition is 60–70%. (The greater cathodic efficiency deduced in respect of the pure zinc system is a consequence of the diverging Tafel lines for hydrogen evolution, Fig. 1.) Hence, the anodic inhibition is again considerably more than expected whilst the cathodic inhibition is considerably less. This trend is apparent even more strikingly when A_e and ϕ_e values are compared, since the latter are very much more sensitive to small variations in i than ϕ_p in the range $\phi_p \to 1$ and $\phi_e \to 0$.

It is only possible to speculate at present about the cause of the above anomaly. Further progress can only be made by careful consideration of the mechanisms of the individual zinc dissolution and hydrogen evolution processes and by establishing how these are likely to be modified other than by a simple blocking action in the presence of the separator. In the case of the zinc dissolution process summarized (Equations 4–6) the rate determining step is step 2 (Equation 5). This is an *electron-transfer* step between zinc species which reside close to the electrode surface. There is some evidence from detailed low-frequency, inductive impedance spectra that Zn(I) is adsorbed particularly in Leclanché electrolyte [17], although to the knowledge of the authors these studies have not been extended to amalgamated zinc. The impedance of zinc in pure NH_4Cl solutions can also show a low-frequency, capacitive loop characteristic of the presence of an adsorbed intermediate when care is taken to eliminate or minimize mass transfer effects [9]. It is therefore possible that the separator material is particularly effective in competing for adsorption sites which might otherwise be occupied by Zn(I) species. In this case a simple 1 : 1 correlation between separator coverage and current inhibition might not be expected. Interestingly, it has been demonstrated from studies of the zinc exchange reaction in Leclanché electrolyte [8] that when step 1 (Equation 4) is rate determining a very good correlation exists between coverage and current inhibition. Step 1 is an *ion-transfer* step involving sites which are fixed on the metal surface thus making a 1 : 1 correlation more likely. Therefore it seems that the separator provides an extra inhibiting power when the reaction involves species which possess some surface mobility. Some credence may be given to this theory in view of the observed differences in separator inhibiting power on pure zinc and amalgamated zinc (Table 2). The ϕ_e values differ by a factor of 4. It is postulated that this large difference results from

Table 2. Parameters derived from high-current (Tafel line) polarization data

Electrode–separator system	*Anodic*							*Cathodic*						
	b_a *(mV)*	i_a *($\mu A\,cm^{-2}$)*	i_a^s *($\mu A\,cm^{-2}$)*	$\Delta\eta$ *(mV)*	ϕ_c	ϕ_p	I_s *(%)*	b_c *(mV)*	i_c *($\mu A\,cm^{-2}$)*	i_c^s *($\mu A\,cm^{-2}$)*	$\Delta\eta$ *(mV)*	ϕ_e	ϕ_p	I_s *(%)*
Zn–paper	30	5400	1150	20	0.213	0.79	79	140	243	138	30	0.568	0.43	43
Zn–methylcellulose–paper	40	5400	32.1	80	0.006	0.99	99	160	243	64	80	0.263	0.74	74
Zn(Hg)–methylcellulose–paper	40	375	9.8	63	0.026	0.98	98	180	8.1	3.2	70	0.395	0.60	60

$E_A = -1.10\,V$; $E_C = -1.28\,V$.

changes in the adsorption characteristics of the Zn(I) species on the two surfaces. Thus, in the case of the Zn(Hg)–methylcellulose–paper system it is possible that the coverage of the zinc surface by intermediates is *lower* than that in the zinc–methylcellulose–paper system. Although compounded by possible surface oxidation in respect of the Zn(Hg) electrode, discussed previously, this theory is also consistent with the fact that the anodic current is always higher for pure zinc than Zn(Hg), both in pure NH_4Cl solutions (cf. Figs 1 and 2) and Leclanché electrolyte [8]. A more strongly adsorbed intermediate Zn(I) in the case of pure zinc, and consequently a lower activation energy for the charge-transfer process, may be responsible. Further work is clearly necessary in order to clarify the situation.

Although it is possible to approach an explanation for the excessive inhibition of the zinc dissolution process, it is very much more difficult to understand the deficient inhibition of hydrogen evolution. In NH_4Cl solutions the latter reaction involves the reduction of NH_4^+ ions [2] which in the absence of specific adsorption reside at the outer Helmholtz plane. The results obtained in the present work suggest that the number of NH_4^+ ions present in this pre-electrode layer could be much less affected by the presence of the separator than expected from the reduction in the geometrical electrode area. Earlier work in Leclanché electrolyte showed that the double-layer capacity is not affected in any systematic way by the presence of methylcellulose. Table 3 confirms that in pure NH_4Cl also, the presence of methylcellulose does not cause changes in the double layer capacity of either pure zinc or amalgamated zinc. However, these results are very difficult to reconcile with the observation that *some* inhibition of hydrogen evolution, albeit less than expected, does occur. This suggests that other factors may be more relevant. Thus it is possible that as a result of its small size and high mobility, the proton is able to penetrate those regions of the metal–separator interface normally inaccessible to bulkier ions. This would have the effect of increasing the ϕ_e value above that expected on the basis of the resistance measurements and the discrepancy with the A_e value could then be accounted for.

4. Comparison of corrosion rates

Table 3 summarizes data derived from low-current measurements at or near the open circuit (corrosion) potential. Data in respect of impedance measurements and polarization measurements are presented separately. Except for the double-layer capacity values, the other parameters are related to the corrosion rate of zinc, and various corrosion currents are tabulated. It must be emphasized, however, that no original information concerning the mechanism of action of the separator is possible by further analysis, since the net corrosion rate is determined by the juxtaposition of the individual anodic and cathodic Tafel lines which have already been analysed and discussed. Nevertheless, it is important to quantify the *overall* effects, particularly those pertinent to the battery environment.

The quoted double-layer capacity values were obtained from the impedance semicircles of Figs 1 and 2 using the relation

$$C_{dl} = 1/2\pi f^* R_{ct} \tag{15}$$

where f^* is the critical frequency at the top of the semicircle. It is seen that the value for pure zinc is $38\,\mu F\,cm^{-2}$ in exact agreement with that deduced previously in 6 M NH_4Cl [6] and also in concentrated (30% w/w) KOH solution [5]. Using a value of $16\,\mu F\,cm^{-2}$ for the capacity of an ideally smooth (mercury) electrode at the minimum of the capacity–potential curve in concentrated solutions, the measured capacity in the present work reflects a roughness factor of ~ 2.5. The capacity is lowered in the presence of the paper, but this lowering is not apparently increased by the presence of the methylcellulose coating. It would be expected that some lowering in capacity would result from the reduced real area of the electrode in the presence of the separator due to its blocking action. However, on this basis the methylcellulose should also produce a fall in capacity, which is

Table 3. Parameters derived from low-current polarization and faradaic impedance data at or near the open-circuit (corrosion) potential

Electrode–separator system	*Impedance data*					*Polarization data*					
	C_{dl} *($\mu F\,cm^{-2}$)*	R_{ct} *($\Omega\,cm^2$)*	R_{dc} *($\Omega\,cm^2$)*	$i_{cor}^{R_{dc}}$ *($\mu A\,cm^{-2}$)*	I_{cor} *(%)*	R_p *($\Omega\,cm^2$)*	$i_{cor}^{R_p}$ *($\mu A\,cm^{-2}$)*	i_{cor}^{ext} *($\mu A\,cm^{-2}$)*	I_{cor} *(%)*	i_{cor}^{bat} *($\mu A\,cm^{-2}$)*	I_{cor}^{bat} *(%)*
Zn	38	113	339	32.0	–	372	29.2	30.7	–	4.7	–
		124	361			380					
Zn–paper	29	364	564	18.6	42	604	17.4	18.4	40	–	–
		363	592			620					
Zn–methylcellulose–paper	29	1698	as R_{ct}	7.7	76	1449	10.0	11.3	63	3.3	30
		1759	as R_{ct}			1490					
Zn(Hg)	13	2007	as R_{ct}	4.2		2500	5.2	3.1	–	0.64	–
		2210	as R_{ct}			2610					
Zn(Hg) -methylcellulose–paper	13	4010	as R_{ct}	1.0	76	6726	2.1	0.8	74	0.25	41
		4176	as R_{ct}			6907					

not observed. A possible cause of this discrepancy has already been discussed. It can be seen that the effect of amalgamation is to reduce the capacity of the bare metal surface by 65%. This can be attributed to the presence of the non-passivating film discussed earlier and confirms earlier work using a different (electrodeposition) method of amalgamation where a similar fall in capacity was observed [6].

Corrosion currents were deduced from impedance measurements using R_{dc} values and the relation of Stern and Geary [18, 19] where

$$R_{dc} = R_{\omega=0} \tag{16}$$

and

$$i_{cor} = (1/2.3R_{\omega=0})\,[b_a b_c/(b_a + b_c)] \tag{17}$$

It can be seen from Table 3 that the reproducibility between R_{dc} values is generally good. Values of $i_{cor}^{R_{dc}}$ represent the mean of the two experimental determinations. Using these corrosion currents, corrosion inhibition factors, I_{cor}, were determined using the relation

$$I_{cor} = 100\,[1 - (i_{cor}^{s}/i_{cor})] \tag{18}$$

Low-current polarization data was also analysed to obtain corrosion currents. This was achieved in two ways. Firstly, from R_p, where

$$R_p = (dE/di)_{i\to 0} = R_{\omega=0} \tag{19}$$

followed by substitution in Equation 17 to yield $i_{cor}^{R_p}$. Secondly, from the extrapolation of Tafel lines to yield i_{cor}^{ext}. Values $i_{cor}^{R_p}$ and i_{cor}^{ext} represent the mean of two experimental determinations. Values of I_{cor} have also been determined using i_{cor} in Equation 18. It can be seen that reproducibility between R_p values is again satisfactory.

A comparison of the corrosion currents derived from the impedance and polarization techniques yields a reasonable agreement confirming the internal consistency of the methods employed and providing further credence to the quoted values. It can be seen that the paper separator alone inhibits the corrosion rate of pure zinc by 40–42% (mean value 41%), whereas the complete separator formulation inhibits the corrosion rate of pure zinc by 63–76% (mean value 70%) and amalgamated zinc by 74–76% (mean value 75%). This reinforces the view that an ostensibly blocking-type mechanism is responsible for the inhibition. It must be emphasized, however, that these inhibition factors are strictly relevant for the case of zinc corroding in electrolyte devoid of any appreciable concentration of zinc ions. In this situation the open-circuit (mixed) potential is free to vary appreciably in response to unequal changes in the position of the individual anodic and cathodic Tafel lines. In a battery environment, however, where the concentration of zinc ions is very high, the open-circuit potential approximates to a reversible potential (particularly in respect of amalgamated zinc) and will be approximately constant, since it will be related to the zinc ion activity via the Nernst equation. This is borne out in practice [8]. Therefore, in order to estimate corrosion inhibition factors which are likely to be relevant in the battery environment, it is necessary to extrapolate the *cathodic* branches of the polarization curves in Figs 1 and 2 to the pertinent potential of zinc in battery electrolyte ($E \approx -1.06$ V). The last two columns in Table 3 provide data in respect of these extrapolations. It can be seen that this procedure reduces the efficiencies for corrosion inhibition afforded by the complete separator formulation from 70 to 30% for pure zinc and from 75 to 41% for amalgamated zinc, which is a reduction of a little over and a little under 50%, respectively.

5. Conclusions

1. The polarization and impedance characteristics of zinc immersed in flooded 6 M NH_4Cl solutions,

either in the presence or absence of the separator, can be interpreted almost exclusively in terms of charge transfer effects.

2. In the presence of the base paper only, the rate of the anodic zinc dissolution process is inhibited by 79% whilst the rate of the cathodic hydrogen evolution process is inhibited by 43%. The anodic reaction inhibition is 13% *greater* than that predicted on the basis of a simple blocking type model, namely 66%, whilst the cathodic reaction inhibition is 23% *less*.

3. In the presence of the complete methylcellulose–paper separator formulation the rate of the anodic zinc dissolution process is inhibited by 98–99% whilst the rate of the cathodic hydrogen evolution process is inhibited by 60–74%. The anodic reaction inhibition is again *greater* than predicted on the basis of a simple blocking type model, namely 89%, whilst the cathodic reaction inhibition is again considerably *less*.

4. The zinc dissolution reaction in 6 M NH_4Cl solution either in the presence or absence of the separator involves two consecutive one-electron transfers with step 2 rate determining

$$\mathrm{Zn} \rightleftharpoons \mathrm{Zn(I)} + e \qquad \text{step 1}$$

$$\mathrm{Zn(I)} \longrightarrow \mathrm{Zn(II)} + e \qquad \text{step 2 (r.d.s.)}$$

It is postulated that the excessive inhibition of step 2 in the presence of the separator, over and above that predicted on the basis of a blocking mechanism, may result from an additional effect on the stability and adsorption characteristics of the Zn(I) species. Differences in the inhibition of the dissolution process on pure zinc and amalgamated zinc together with differences in the absolute magnitude of the zinc dissolution current tend to support this view and suggest that Zn(I) may be much less strongly adsorbed on zinc (Hg) than on pure zinc.

5. The deficient inhibition of the cathodic process may result from the small size and high mobility of the proton which allows it to penetrate those regions of the metal–separator interface normally inaccessible to bulkier ions. However, other mechanisms probably participate.

6. The corrosion inhibiting efficiency of the base paper only on pure zinc has a mean value of 41%. The corrosion inhibiting efficiency of the complete separator formulation has a mean value of 70% for pure zinc and 75% for amalgamated zinc. A translation of this latter behaviour to the complete battery environment, however, predicts values of 30% and 41%, respectively. This represents a reduction of a little over and a little under 50%, respectively, compared with the situation in the flooded electrolyte.

Acknowledgement

The authors wish to thank the Directors of British Ever Ready Ltd, for permission to publish this work.

Appendix

Determination of volume fractions, tortuosity factors and area fractions from ohmic impedance data

The derivations which follow are based on the conclusions from a general model of the separator region discussed by Tye [14]. In this model the separator is represented as an assembly of conducting pores. It is further assumed that the current flow is constant throughout its length and that the area of the pore normal to the direction of current is also constant throughout the length of the pore. The volume fractions, tortuosities and area fractions are 'averaged' values for all pores. Calculation of these parameters from experimental impedance data is facilitated by the technique of maintaining the Luggin reference probe at a *constant* distance from either the free electrolyte exposed (outer)

surface of the separator (experiments with separators) or the zinc surface (experiments without separators). This technique is described in the Experimental section.

Paper separators. Complex impedance diagrams (R_s versus $1/\omega C_s$) determined in the presence and absence of the separator were first extrapolated to the resistive axes $(Z)_{\omega=\infty}$ to yield the values R_Ω^s and R_Ω, respectively. These values were then corrected for electrode area to yield units in $\Omega\,cm^2$. The resistance of electrolyte within the paper, r_p, was determined by subtraction

$$r_p = R_\Omega^s - R_\Omega \tag{A1}$$

and the resistance of 'free' electrolyte, having an equivalent geometry and volume to that of the separator, r_e, was determined from the expression

$$r_e = R_\Omega\,(t_p/x) \tag{A2}$$

Now,

$$r_p/r_e = \bar{\varrho}/\varrho = \theta^2/V_e \tag{A3}$$

Here

$$\theta = l/t_p \tag{A4}$$

Furthermore, the area fraction of electrolyte adjacent to the zinc, A_e, follows from a knowledge of V_e and θ, since

$$A_e = V_e/\theta \tag{A5}$$

Coated paper separators. In experiments with coated paper separators, only parameters relating to the *coating* are of relevance as far as the charge-transfer reactions are concerned, since it is only the coating layer which is in direct contact with the zinc surface. Complex impedance diagrams determined in the presence of either the coated paper, the uncoated paper or in the absence of any separator, were first extrapolated to the resistive axes to yield the values R_Ω^s, R_Ω^p and R_Ω, respectively. The resistance of electrolyte within the coating layer was determined by subtraction

$$r_c = R_\Omega^s - R_\Omega^p \tag{A6}$$

and the resistance of free electrolyte having an equivalent geometry and volume to that of the coating layer, r_e, was determined from the expression

$$r_e = R_\Omega\,(t_c/x) \tag{A7}$$

Determination of V_e, θ and A_e then follows as described in the Appendix above and in the text.

References

[1] L. M. Baugh, *Electrochim. Acta* **24** (1979) 657.
[2] *Idem, ibid.* **24** (1979) 669.
[3] L. M. Baugh, R. J. Field and J. A. Lee, *ibid.* **25** (1980) 751.
[4] L. M. Baugh, P. M. Gidney and J. A. Lee, *ibid.* **25** (1980) 765.
[5] L. M. Baugh, F. L. Tye and N. C. White, in 'Power Sources 9' (edited by J. Thomson), Academic Press, London (1983) p. 303.
[6] *Idem, J. Appl. Electrochem.* **13** (1983) 623.
[7] L. M. Baugh and A. Higginson, *J. Power Sources* **13** (1984) 297.
[8] L. M. Baugh and N. C. White, paper presented at 15th International Power Sources Symposium, Brighton, UK, September, 1986, to be published in 'Power Sources II' (edited by L. Pearce) (1987).
[9] *Idem, J. Appl. Electrochem.* **17** (1987) 1037.
[10] C.R.C. Handbook of Chemistry and Physics, 57th Edn, C.R.C. Press, (1977).
[11] L. M. Baugh and A. Higginson, *Electrochim. Acta* **30** (1985) 1163.

[12] T. Hurlen and K. P. Fischer, *J. Electroanal. Chem.* **61** (1975) 165.
[13] J. O'M. Bockris, Z. Nagy and A. Damjanovic, *J. Electrochem. Soc.* **119** (1972) 285.
[14] F. L. Tye, *Chem and Ind.*, May (1982) 322.
[15] J. A. Lee, W. C. Maskell and F. L. Tye, in 'Membrane Separation Processes' (edited by P. Meares), Elsevier, Amsterdam (1976) p. 425.
[16] A. Agopsowicz, R. Brett, J. E. A. Shaw and F. L. Tye in Power Sources 5 (edited by D. H. Collins), Academic Press, London (1975) p. 503.
[17] C. Cachet and R. Wiart, *J. Electroanal, Chem* **111** (1980) 235.
[18] M. Stern and A. L. Geary, *J. Electrochem. Soc.* **104** (1957) 56.
[19] M. Stern, *Corrosion* **14** (1958) 440.